

# Electrochemical capacitors with plasticized gel-polymer electrolytes

S. Mitra<sup>a</sup>, A.K. Shukla<sup>b</sup>, S. Sampath<sup>a,\*</sup>

<sup>a</sup>Department of Inorganic and Physical Chemistry, Indian Institute of Science, Bangalore 560012, Karnataka, India

<sup>b</sup>Solid State Structural Chemistry Unit, Indian Institute of Science, Bangalore 560012, Karnataka, India

Received 18 December 2000; accepted 31 January 2001

## Abstract

Solid electrolytes which comprise lithium and magnesium triflate ionic salts in polyacrylonitrile (PAN)-based gels are used to fabricate electrochemical double-layer capacitors in conjunction with ethylene carbonate (EC) and propylene carbonate (PC) as plasticizers and high-density graphite (HDG) as polarizable electrodes. The conductivity of the solid electrolytes is around  $10^{-3}$  S  $\text{cm}^{-1}$  at ambient temperatures. Composites which consist of PAN + EC + PC + electrolyte are electrochemically stable over a wide potential range. Cells of the type: HDG/PAN-EC-PC-Li and Mg-triflate/HDG exhibit single-electrode discharge capacitance values of 480 and 383  $\mu\text{F cm}^{-2}$ , respectively, with attractive charge-discharge characteristics. © 2001 Elsevier Science B.V. All rights reserved.

**Keywords:** Magnesium ion conductor; Solid electrolyte; Polymer-gel; Electrochemical capacitor; High density graphite; Power source

## 1. Introduction

In recent years, electrochemical capacitors for reversible electrical energy-storage and delivery have been developed for a number of applications. Electrochemical capacitors are complementary to secondary batteries and offer applications primarily in hybrid-power systems for electric vehicles, utility load-maintenance, cold-start assist, and memory back-up systems [1]. The energy-storage mechanism in electrochemical capacitors is based on the separation of charges at the interface between a solid electrode and an electrolyte, and/or fast reactions at the interface that are pseudo-faradaic in nature.

An effective method of fabricating electrochemical double-layer capacitors with high power-density is to use a thin-layer solid electrolyte [2]. Parameters, such as low conductivity, poor contact, presence of crystalline domains, high internal-resistance and low mechanical-strength limit, however, the use of solid polymer electrolytes in electrochemical capacitors. Organic solvent-based polymer electrolytes with high stability have been recently reported [2–5] to be favorable materials for this purpose. In addition, gel electrolytes based on a combination of polyethylene oxide (PEO), polymethylmethacrylate (PMMA) and propylene

carbonate (PC) with lithium perchlorate salt have been reported by Ishikawa et al. [6]. These gels are superior to solid polymer-electrolytes based on PEO which contains lithium salts in terms of their conductivity, and they also possess adequate mechanical strength. Nevertheless, PEO-lithium perchlorate solid-polymer electrolytes have high internal-resistance at ambient temperatures, which makes them unattractive for several applications. Ishikawa et al. [5] have examined the use of polymer-gel electrolytes based on polyacrylonitrile (PAN) and PC for capacitor applications. Matsuda et al. [4] have studied polyvinylpyrrolidone (PVP), polyvinyl-acetate (PVA) and PC-based gel-electrolytes for this purpose. The ionic dispersants used in most of these studies comprise salts such as lithium perchlorate [3,7], tetrabutylammonium perchlorate tetraethylammonium perchlorate, and tetraethylammonium flouoroborate [5].

Proton conducting polymer-electrolytes [8,9] based on  $\text{HClO}_4$  and  $\text{H}_3\text{PO}_4$  have also been attempted with capacitance values similar to those obtained with a liquid electrolyte. The power density of these capacitors is limited, however, by an operating voltage-window of only about 1 V. Solid electrolytes which exhibit ionic conduction other than protons are, therefore, desirable. Accordingly, efforts are being made to find electrolytes which have adequate ionic conductivity under ambient conditions and a large operating voltage-window.

Among the polymer matrices, donor polyether solvents, such as PEO, in which anions are usually not co-ordinated to the solvent molecules unless otherwise through hydrogen

\* Corresponding author. Tel.: +91-80-3092825;  
fax: +91-80-3600683/+91-80-3601552.  
E-mail address: sampath@ipc.iisc.ernet.in (S. Sampath).

bonding to hydroxyl-end groups, are quite frequently used as solid electrolytes along with a plasticizer. The binding capacity of the commonly used anions in preparing polymer-salt complexes in aprotic solvents varies in the order:  $\text{SCN}^- > \text{I}^- > \text{ClO}_4^- > \text{CF}_3\text{SO}_3^-$  [10,11]. It is also reported that the triflate anion has a strong tendency for 'structure breaking' in an aprotic medium and that this would overcome the 'structure making' characteristics of cations such as  $\text{Li}^+$  and  $\text{Na}^+$ . Accordingly, the solvent matrix would be disrupted with a concomitant increase in disorder [12,13]. This, in turn will increase the amorphicity of the medium that is desirable to increase the conductivity. It is noteworthy, however, that ion association based on entropy considerations would lead to a larger number of ion pairs at elevated temperatures [14]. Hence, triflate salts could be used as electrolytes provided a high ionic-conductivity is achieved in the solid matrix at ambient temperatures. The PAN-based gel electrolytes have been proposed as an alternative to PEO-based systems [15,16] which provide high conductivity and good mechanical properties, such as ease of fabrication, high flexibility, and low density. As for the electrode materials, various types of activated carbon powders and high-density graphite (HDG) have been employed in the fabrication of electrochemical capacitors.

In this work, we report the characteristics of electrochemical capacitors fabricated by using PAN-based solid polymer-gel electrolytes that contain magnesium (or lithium) triflate salt sandwiched between HDG discs. In the literature, divalent and trivalent cations as mobile species in polymeric electrolytes have not been explored in detail [17–22]. Magnesium triflate based gel-polymer electrolytes exhibit adequately high conductivities of the order of  $10^{-3} \text{ S cm}^{-1}$  at ambient temperatures. To our knowledge, this study is first of its type on magnesium-based electrolytes as capacitor materials.

## 2. Experimental

### 2.1. Materials

Polyacrylonitrile (PAN; molecular weight 86,200), ethylene carbonate (EC), propylene carbonate (PC), lithium and magnesium triflate (trifluoromethanesulfonate) were obtained from Aldrich, USA.

### 2.2. Preparation of gel electrolytes and electrochemical capacitors

The solvents (EC and PC) were distilled under vacuum prior to their use. The required quantity of metal salt was first dissolved in a mixture of EC and PC (1:1 by weight). PAN was added to this mixture and the suspension was heated to  $120^\circ\text{C}$  with stirring until the polymer dissolved to yield a homogeneous solution. The resulting viscous solution was cast on a glass plate and allowed to cool down to room

temperature to obtain the electrolyte in a film form (150–300  $\mu\text{m}$  thickness). The thickness of the solid electrolyte was measured using a Digimetric micrometer. Equal amounts of EC and PC (weight ratio: 2.5 times that of EC and PC to PAN) with respect to PAN were used in all the experiments. Typically, preparation of the electrolyte involves the use of PAN (1 g), EC (2.5 g), PC (2.5 g) and 0.1 mol% metal salt (0.16 g in the case of lithium triflate and 0.32 g for magnesium triflate). The electrolyte films, cut to the size of the HDG (1 mm thick,  $0.50 \text{ cm}^2$  geometric area, surface area  $0.305 \text{ m}^2 \text{ g}^{-1}$  and specific gravity  $3.36 \text{ cm}^{-3}$ ) electrodes were stored in a vacuum desiccator.

### 2.3. Electrochemical characterization

Electrochemical capacitors were constructed with either PAN-gel-lithium triflate or PAN-gel-magnesium triflate electrolyte sandwiched between two polished HDG electrodes. Electrical contact between the HDG and the current-collector was made by silver conductive paste. The capacitor performance was characterized by ac impedance spectroscopy, cyclic voltammetry, and galvanostatic charge-discharge measurements at various current densities [23]. Impedance spectroscopy and cyclic voltammetry were carried out using an EG&G PARC-273 potentiostat interfaced with a EC-5210 lock-in amplifier or using an Auto Lab Electrochemical system (The Netherlands). Constant-current charge-discharge measurements were carried out with a CH-660A electrochemical system, USA. The bulk electrical conductivity of the electrolyte determined from complex impedance spectra in the temperature range  $25\text{--}80^\circ\text{C}$ . The frequency range used was 100 kHz to 100 mHz with a perturbation of 5 mV rms at 0 V dc bias conditions. The capacitance values,  $C$ , for a single electrode were calculated from the impedance data using the following equation:

$$C = -\frac{1}{Z_{\text{img}}\omega} \quad (1)$$

where  $\omega$  is the angular frequency and  $Z_{\text{img}}$  the imaginary component of the total impedance ( $Z$ ). Capacitance values were calculated at a frequency of 100 mHz.

Cyclic voltammograms were carried out in the potential range  $+0.8$  to  $-0.8$  V with different scan rates using a two-electrode configuration. The charge-discharge behavior of the capacitors was followed galvanostatically at different constant current densities between 0.2 and  $2 \text{ mA cm}^{-2}$  for various cycles. The real capacitance and the integrated capacitance were calculated from discharge curve using the following equations:

$$C(\text{real}) = -\frac{I}{dE/dt} \quad (2)$$

$$C(\text{integrated}) = \frac{I \Delta t}{\Delta V} \quad (3)$$

where  $I$  is the constant current,  $\Delta t$  the time required to

change the potential by  $\Delta V$ ,  $dE/dt$  the slope of the linear portion of the discharge curve. The coulombic efficiency ( $\eta$ ) was calculated at a constant current density using the equation:

$$\eta = \frac{t_d}{t_c} \times 100 \quad (4)$$

where  $t_d$  and  $t_c$  are the times taken for discharging and charging of the capacitor, respectively.

### 3. Results and discussions

#### 3.1. Electrical conductivity of the gel-polymer electrolytes

The PAN-based electrolytes which comprised PAN–EC–PC and magnesium (or lithium) triflate were isolated as free-standing films with thicknesses of the order of 150–250  $\mu\text{m}$ . The films were transparent. It was found that the solubility of the ionic dispersant depends on the amounts of EC and PC in the films, but the mechanical stability depends on the amount of PAN present in the film. The composition of the gel-polymer electrolyte was optimized in order to get mechanically-stable films with good conductivity. A typical composition used in the present studies is 16 wt.% PAN; 40 wt.% EC; 40 wt.% PC; 0.1 mol% of inorganic salt. The conductivity of the PAN-based film  $\sigma$ , was calculated as follows:

$$\sigma = \frac{l}{RA} \quad (5)$$

where  $l$  is the thickness of the film and  $R$  the bulk resistance of the electrolyte which can be obtained from the high-frequency intercept on the  $Z'$  axis of the Cole–Cole plot. The temperature dependence of the electrical conductivity of lithium triflate and magnesium triflate based electrolytes in the temperature range 25–80°C is shown in Fig. 1(a) and (b), respectively. Conductivity measurements were performed on blocking electrodes of configuration SS (stainless steel)/electrolyte/SS. The polymer electrolytes exhibit conductivity values of the order of  $10^{-3} \text{ S cm}^{-1}$  at 25°C. The temperature dependence of conductivity for lithium as well as for magnesium triflate parallels the reported behavior for lithium salts [16]. The activation energies are 0.15 and 0.1 eV for lithium triflate and magnesium triflate based electrolytes, respectively. The low activation energies are consistent with ionic motion facilitated more by solvent than by the segmental motion of the polymer chains. The activation energy values also show that magnesium ions are more mobile than lithium ions in the PAN + EC + PC matrix. This may be due to the solvation being higher in the case of lithium ions than magnesium ions due to the low polarizability of magnesium as compared with lithium based on size and charge considerations.

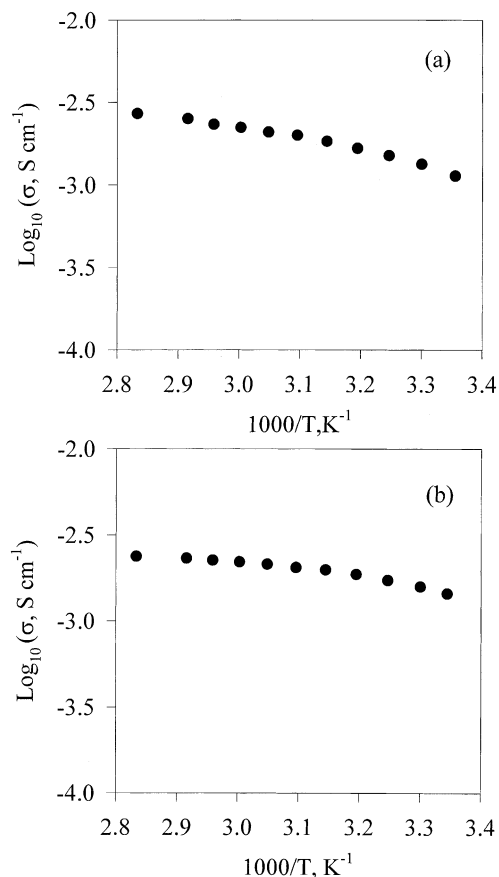


Fig. 1.  $\text{Log}_{10} \sigma$  vs.  $10^{-3}/T$  plot for: (a) SS/PAN gel–Li–triflate/SS system; (b) SS/PAN gel–Mg–triflate/SS system.

#### 3.2. Characterization of electrochemical capacitors

The ac impedance response of capacitors assembled with two polymer-gel electrolytes at 80°C are shown in Fig. 2(a) and (b). In the case of the magnesium triflate based gel electrolyte (Fig. 2(b)), the Cole–Cole plots show a blocking behavior at all temperatures. No semicircle was observed in the high frequency region at any of the temperatures studied. On the other hand, the lithium triflate based gel electrolyte displays blocking behavior at low temperatures but a semicircle is obtained at high temperatures (Fig. 2(a)). This semicircle may be due to the intercalation of lithium ions into the HDG electrode or ion-diffusion in the pores of the HDG which gives a high inner electrolyte resistance that manifests at higher temperatures.

The frequency-dependent phase angle plots for each capacitor is shown in Fig. 3. Typically, values around  $\sim 76^\circ$  in the frequency range 10–100 mHz are observed. This demonstrates the good capacitive behavior exhibited by the HDG/PAN–triflate interface. Single-electrode capacitance values calculated from the impedance spectra are 0.429 and 0.388  $\text{mF cm}^{-2}$  at 25°C for the lithium triflate and magnesium triflate based capacitors, respectively. The capacitance values increase with increasing temperature for both gel electrolytes (Fig. 4). This is probably due to the

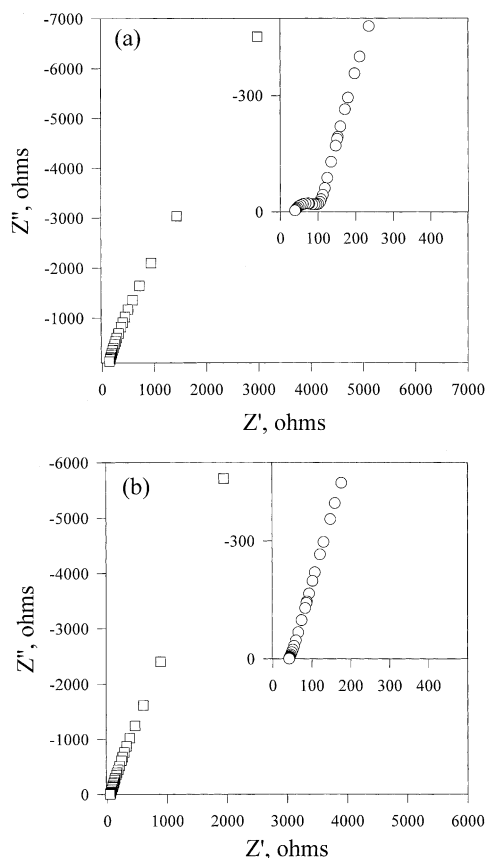


Fig. 2. (a) Typical ac impedance plot for: (a) HDG/PAN gel-Li-triflate/HDG system at 80°C, inset shows expanded high-frequency region; (b) HDG/PAN gel-Mg-triflate/HDG system at 80°C, inset shows expanded high-frequency region.

faster movement of ions which causes a decrease in the bulk resistance of the gel. A change in the physical state of the PAN films with increase in temperature to give a better contact at the HDG–electrolyte interface may also lead to

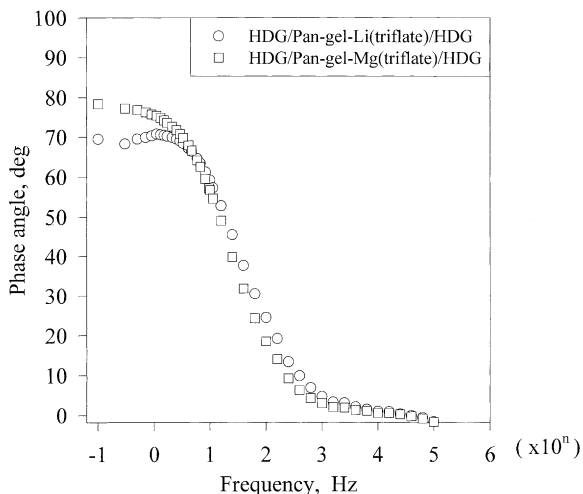


Fig. 3. Phase angle vs. frequency plots at 25°C.

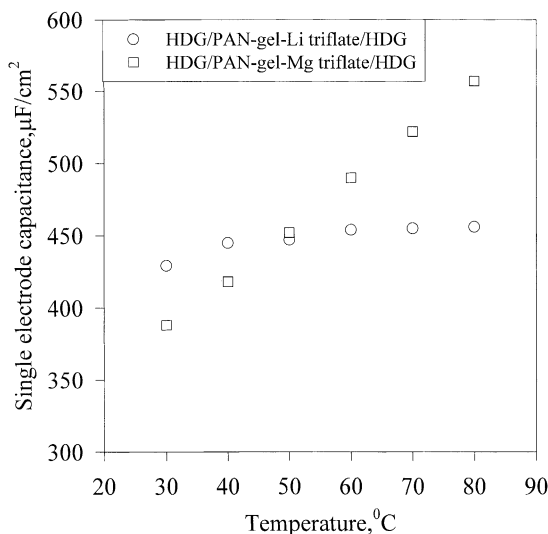


Fig. 4. Temperature dependence of single electrode capacitance calculated from ac impedance data at 100 mHz frequency.

such a behavior. This is supported by the data for the temperature dependence of the elastic modulus and loss tangent [24]. It also been reported [18] that that the physical state of hybrid PAN-films which contain plasticizers changes on increasing the temperature. The glass-transition temperature ( $T_g$ ) is lowered by the presence of plasticizer as well as the salt. As expected, the bulk resistance obtained from the high-frequency intercept on the complex-plane plot decreases with increasing temperature for both electrolytes. By contrast, the charge-transfer resistance obtained from the low frequency intercept is high for the HDG/PAN–gel–lithium triflate interface at 80°C. It is noteworthy that a clear semicircle is formed in the complex plane plot for the HDG/PAN–gel–lithium triflate interface at 80°C whereas the magnesium triflate based electrolyte/HDG interface does not exhibit such behavior at the same temperature.

Cyclic voltammograms for HDG/PAN–gel–lithium triflate/HDG and HDG/PAN–gel–magnesium triflate/HDG cells at a scan rate of  $0.6 \text{ V s}^{-1}$  for the 1st and 50th cycles at 25°C are shown in Fig. 5. The almost featureless characteristics of the voltammograms indicate that the electron transfer between the electrode and the gel-electrolyte occurs at a constant rate, giving a fairly perfect mirror image between the charging and the discharging process. It would be noted, however, that the voltammograms of the lithium salt–gel-based capacitor shows a small hump at 0.3 V. This may be attributed to intercalation or diffusion of ions into the microscopic rough surface (pores) of the HDG electrode. The inset in Fig. 5 shows the potential window of the PAN–gel–magnesium salt-based electrolyte. The experiment was carried out using a three-electrode configuration at 25°C. The potential window is  $\pm 2.5 \text{ V}$  which is in agreement with a previous report of the PAN–gel–lithium salt system [9]. The capacitance values for cells based on both electrolytes, calculated from the capacitive currents and scan rate,

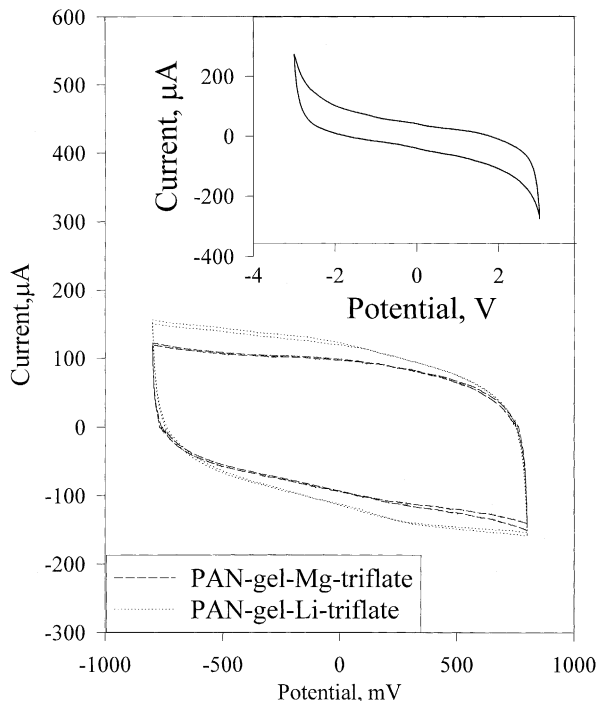


Fig. 5. Cyclic voltammograms (1st and 50th cycles) of HDG/PAN-gel electrolyte/HDG system at scan rate of  $0.6 \text{ V s}^{-1}$  at  $25^\circ\text{C}$ . Inset shows potential window of PAN-gel-Mg triflate system with SS electrodes at  $25^\circ\text{C}$ .

agree well with the values obtained from charge–discharge experiments.

### 3.3. Leakage-current measurements

Leakage-current measurements were performed at different applied potentials and at  $25^\circ\text{C}$  using the configuration HDG/PAN-gel-Mg salt/HDG. The variation of leakage current with applied voltage is presented in Fig. 6. The leakage current gradually increased with increasing applied voltage. After a certain applied dc bias, a steep increase is observed. This potential is usually termed the ‘cut-off’ potential. In the present studies, PAN-gel-based electrolytes show a cut-off voltage of 2.5 V and this value agrees with the results obtained from cyclic voltammetry for the decomposition of  $-\text{CN}$  groups. Hence, the cut-off voltage for charge–discharge measurements was fixed as  $\pm 2.5 \text{ V}$ .

### 3.4. Charge–discharge characteristics

Galvanostatic charge–discharge experiments were conducted on the two types of capacitors at various current densities. The charge–discharge curves at a constant current density of  $1.2 \text{ mA cm}^{-2}$  at  $25^\circ\text{C}$  are given in Fig. 7. The initial sharp change in potential with time, during both charging and discharging processes, is due to an ohmic-loss which arises from the internal resistance of the cells. The variation of the real and the integrated capacitance with

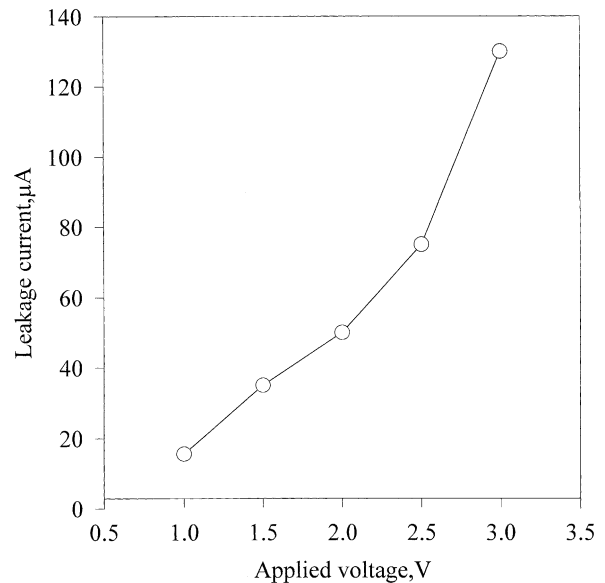


Fig. 6. Leakage current vs. applied voltage for HDG/PAN gel-Mg-triflate/HDG system at  $25^\circ\text{C}$ .

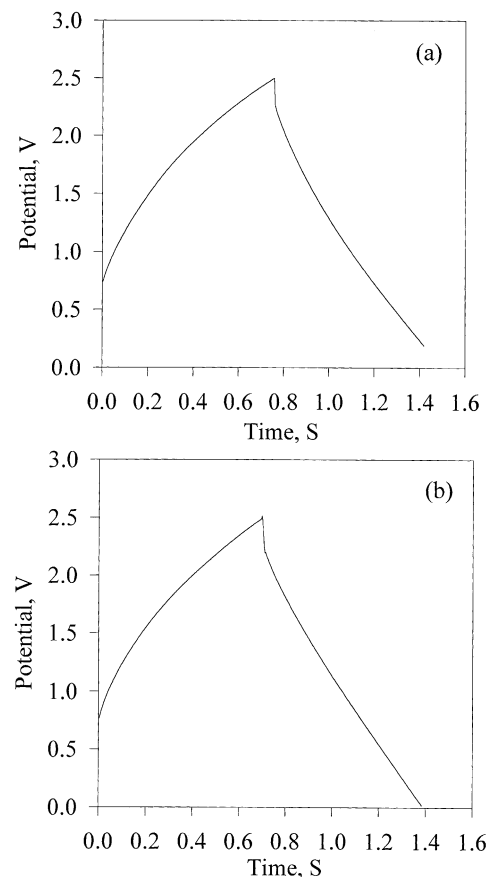


Fig. 7. Charge–discharge curves at current density of  $1.2 \text{ mA cm}^{-2}$  and at  $25^\circ\text{C}$  for: (a) HDG/PAN gel-Li-triflate/HDG system; (b) HDG/PAN gel-Mg-triflate/HDG system.

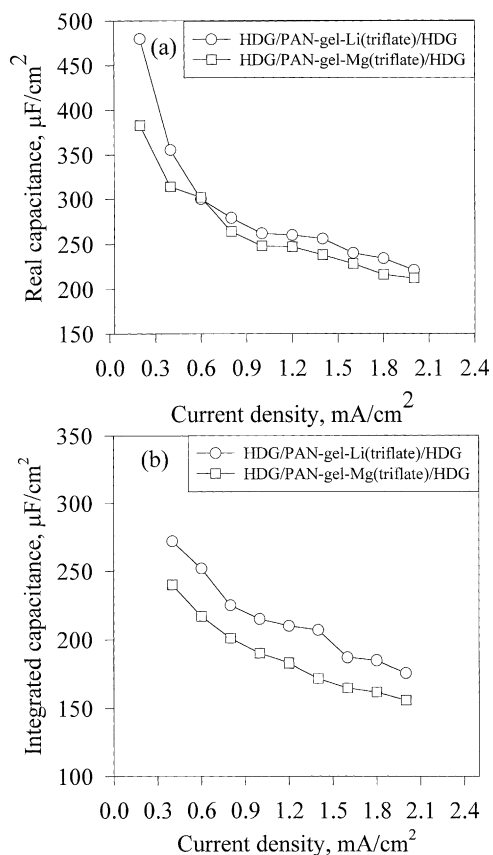


Fig. 8. Variation of (a) real capacitance (calculated from discharge curve); (b) integrated capacitance (calculated from discharge curve) with current density at 25°C.

current density at 25°C is shown in Fig. 8. The capacitance decreases with increasing current density. Liu and Osaka [3] reported similar behavior for capacitors which comprised PMMA–PAN–gel–LiClO<sub>4</sub> electrolyte. As the current density increases, the time required to attain the cut-off voltage of 2.5 V decreases and this probably affects the double-layer formation and leads to a decrease in capacitance.

The coulombic efficiency ( $\eta$ ) was calculated using charge–discharge experiments for both cells at 25°C. The efficiency for the HDG/PAN–gel–Mg salt/HDG cell is 82.9% at 0.4 mA cm<sup>-2</sup>, 90.2% at 0.8 mA cm<sup>-2</sup>, and 90.2% at 2 mA cm<sup>-2</sup>. It is also noteworthy that capacitors charged to 2.5 V at a relatively high current density of 0.8 mA cm<sup>-2</sup>, take about 7 h for complete self-discharge.

#### 4. Conclusion

The results of the recent study suggest that PAN-based gels with monovalent as well as divalent cations could be

used as potential electrolytes for carbon-based electrochemical capacitors. Further studies to understand the effect of various parameters, such as salt concentration, thickness of the electrolyte and other divalent cationic triflates on the behavior of double-layer capacitors based on PAN-based gels are in progress. Studies on capacitors based on high surface-area, activated carbon electrodes are also being pursued.

#### Acknowledgements

We thank the Ministry of Non-conventional energy sources New Delhi, India for financial support.

#### References

- [1] B.E. Conway, *Electrochemical Supercapacitors: Scientific Fundamentals and Technological Applications*, Kluwer-Plenum Publishing Co., New York, 1999.
- [2] X. Liu, I. Momma, T. Osaka, *Chem. Lett.* (1996) 625.
- [3] X. Liu, T. Osaka, *J. Electrochem. Soc.* 144 (1997) 3066.
- [4] Y. Matsuda, K. Inoue, H. Takeuchi, Y. Okuhama, *Solid State Ionics* 113–115 (1998) 103.
- [5] M. Ishikawa, M. Ihara, M. Morita, Y. Matsuda, *Electrochim. Acta* 13–14 (1995) 2217.
- [6] M. Ishikawa, M. Morita, M. Ihara, Y. Matsuda, *J. Electrochem. Soc.* 141 (1994) 1730.
- [7] X. Liu, T. Osaka, *J. Electrochem. Soc.* 143 (1996) 3982.
- [8] J.C. Lassegues, J. Grondin, T. Becker, L. Servent, M. Hernandez, *Solid State Ionics* 77 (1995) 311.
- [9] A. Matsuda, H. Honjo, M. Tatsumisago, T. Minami, *Solid State Ionics* 113–115 (1998) 97.
- [10] A.J. Parker, *Quart. Rev. Chem. Soc. (London)* 16 (1962) 163.
- [11] I. Nwankwo, D.W. Xia, J. Smid, *J. Polym. Sci., Polym. Phys.* 26 (1988) 581.
- [12] S. Schantz, L.M. Torell, J.R. Stevens, *J. Chem. Phys.* 94 (10) (1991) 6862.
- [13] W. Wixwat, Y. Fu, J.R. Stevens, *Polymer* 32 (1991) 1181.
- [14] M.A. Ratner, A. Nitzan, *Faraday Discuss. Chem. Soc.* 88 (1989) 19.
- [15] K.M. Abraham, M. Alamgir, *J. Electrochem. Soc.* 137 (1990) 1657.
- [16] H.S. Choe, B.G. Carroll, D.M. Pasquariello, K.M. Abraham, *Chem. Mater.* 9 (1997) 369.
- [17] F.M. Gray, *Solid Polymer Electrolytes*, VCH, Weinheim, 1991, Chapter 7, p. 125.
- [18] R. Hug, G. Chiodelli, P. Ferloni, A. Magistris, G.C. Farrington, *J. Electrochem. Soc.* 135 (1988) 524.
- [19] F.B. Dias, S.V. Batty, A. Gupta, G. Ungar, J.P. Voss, P.V. Wright, *Electrochim. Acta* 43 (1998) 1217.
- [20] C. Liebenow, *Electrochim. Acta* 43 (1998) 1253.
- [21] L.L. Yang, R. Hug, G.C. Farrington, *Solid State Ionics* 18/19 (1986) 291.
- [22] P.G. Bruce, F.M. Gray, C.A. Vincent, *Solid State Ionics* 38 (1990) 231.
- [23] P.J. Mahon, G.L. Paul, S.M. Keshishian, A.M. Vassallo, *J. Power Sources* 91 (2000) 68–76.
- [24] M. Watanabe, M. Kanba, K. Nagaoka, I. Shinohara, *J. Polym. Sci., Polym. Phys.* 21 (1983) 939.